World Academy of Science, Engineering and Technology
International Journal of Structural and Construction Engineering
Vol:15, No:6, 2021

Experimental Study on the Variation of Young's Modulus of Hollow Clay Brick Obtained from Static and Dynamic Tests

M. Aboudalle, Le Btth, M. Sari, F. Meftah

***Abstract*—**In parallel with the appearance of new materials, brick masonry had and still has an essential part of the construction market today, with new technical challenges in designing bricks to meet additional requirements. Being used in structural applications, predicting the performance of clay brick masonry allows a significant cost reduction, in terms of practical experimentation. The behavior of masonry walls depends on the behavior of their elementary components, such as bricks, joints, and coatings. Therefore, it is necessary to consider it at different scales (from the scale of the intrinsic material to the real scale of the wall) and then to develop appropriate models, using numerical simulations. The work presented in this paper focuses on the mechanical characterization of the terracotta material at ambient temperature. As a result, the static Young's modulus obtained from the flexural test shows different values in comparison with the compression test, as well as with the dynamic Young's modulus obtained from the Impulse excitation of vibration test. Moreover, the Young's modulus varies according to the direction in which samples are extracted, where the values in the extrusion direction diverge from the ones in the orthogonal directions. Based on these results, hollow bricks can be considered as transversely isotropic bimodulus material.

***Keywords*—**Bimodulus material, hollow clay brick, impulse excitation of vibration, transversely isotropic material, Young's modulus.

I. Introduction

BRICK masonry has been utilized for ages. It is, and always has been, an indispensable part of the construction field [1]. The construction techniques using masonry elements have many advantages, which professionals in the field exploit to their profit: mechanical performance, high durability, reduced execution time, acoustic and thermal insulation, significant reduction of thermal bridges and fire protection [2]. In addition, with the evolution of construction requirements, fired-clay masonry is being proposed in a continuous attempt to provide better solutions in terms of fire resistance, seismic, thermal and acoustic insulation, environment, etc. [3]-[5].

New and innovative solutions are implemented on different aspects: material composition, geometry, baking temperature, assembly technique, etc. [6]. In this context, the theoretical approach is an important step to understand the behavior of masonry (bricks, wall) prior to mass production. It may help to save the time and cost required for several tests and to develop reliable processes that could help in the design of new products, while evaluating the safety of a building that can bear both important mechanical and thermal loads [2].

Being used in structural applications, predicting the performance of clay brick masonry allows a significant cost reduction. The behavior of masonry walls depends on the behavior of their elementary components, such as bricks, joints, and coatings. Therefore, it is necessary to consider it at different scales (from the scale of the intrinsic material to the real scale of the wall) and then to develop appropriate models using numerical simulations.

The work presented in this paper focuses on the mechanical characterization at the scale of the terracotta material at ambient temperature. According to several references [7], [8], the behavior of terracotta is considered as an elastic, brittle material. The divergence of the results shows the interest of studying the Young's modulus obtained from different tests, considering more specific criteria, to optimize the modeling. Therefore, tests were carried out based on the position and orientation of the different brick partitions (external, internal, longitudinal and transversal). This paper presents results of an experimental campaign to determine both the dynamic and static Young's modulus of brick masonry constituents through nondestructive and destructive testing methods. For the reliability of the methods, a robust procedure is described and tested on a series of samples of two different bricks from different manufacturers.

II. Background & Theory

This section presents the theory behind the main testing techniques used in this research. It outlines concepts that are important for the accurate evaluation of non-destructive and destructive test results.

A. Flexural Test

The flexural test is a method of determining the bending properties of a material. It consists of placing a prismatic specimen between two supports and applying a load using a third point or with two points which are called the 3-points flexural test and the 4-points flexural test respectively (Fig. 1). Results are plotted on a stress-strain diagram. The modulus of elasticity is determined from the tangent at the origin of the

Aboudalle, M, is with the National Institute of Applied Sciences (INSA de Rennes), Technical Center for Natural Building Materials (CTMNC), France (e-mail: abou-dalle.m@ctmnc.fr).

Le, Btth, and Sari, M, are with the Technical Center for Natural Building Materials, CTMNC, 17 Street Letellier, 75726 Paris Cedex 15, France (e-mail: le.tth@ctmnc.fr, sari.m@ctmnc.fr).

Meftah, F, is with the National Institute of Applied Sciences (INSA de Rennes), 20 avenue des Buttes de Coëmes, CS 70839, 35708 RENNES Cedex, France (e-mail: fekri.meftah@insa-rennes.fr).

load-displacement curves, using (1) and (2) where L is the length of the specimen, l is the length between the upper supports, b is the width, h is the height, P is the applied force and d is the measured displacement [9].

$$E_{3\ points} = \frac{L^3 \times \Delta P}{4 \times b \times h^3 \times \Delta d} \quad (1)$$

$$E_{4\ points} = \frac{\Delta P}{\Delta d} \times \frac{1}{8bh^3} \times (L-l)(2L^2 + 2Ll - l^2) \quad (2)$$

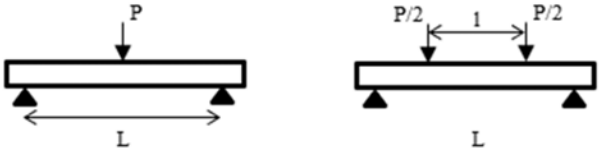

(a) (b)

Fig. 1 (a) 3 points Flexural test, (b) 4 points flexural test

B. Compression Test

The test specimen is placed between two rigid steel plates that uniformly distribute the applied load over the area of its opposite sides sample, and then the stress is gradually increased until the rupture. As the compression stress-strain curve for a typical specimen is initially linear, the modulus of elasticity is determined from the tangent at the origin of the load-displacement curves, using (3) where L is the height of the specimen, A is the area, P is the applied force and d is the measured displacement.

$$Ec = \frac{\Delta P/A}{\Delta d/L} \quad (3)$$

C. Impulse Excitation of Vibration (IEV) Testing

Elastic material specimens have specific mechanical resonant frequencies which are dependent on their density, elastic properties, specimen geometry and boundary conditions imposed by the test device. Therefore, it is possible to calculate the dynamic elastic property of a material if its mass, geometry and mechanical resonance frequencies can be determined. Test devices which identify specific resonance modes as well as the processing of recorded vibration signals make it possible to determine these resonance frequencies (vibration-brick-IEV [10]).

In this paper, a thin prismatic bar assumed to work in flexion is considered. In the (x, y, z) plane, this is equivalent to suppose that:

- $H = L_y << L_x, L_z$ to ensure that only bending modes are excited.
- $L_z >> L_x$, to display only the resonances according to z of the system in low and medium frequencies.

Under these conditions and in a harmonic regime, the deflection y(x) of the system is based on the Bernoulli/Euler equation [11]:

$$\frac{d^4y(x)}{dx^4} = \beta^4\, y(x) \;\; ; \;\; \beta = \frac{\rho A \omega^2}{EI} \quad (4)$$

where ρ is the density, A is the area, ω is the pulsation, E is the Young's modulus, and I is the moment of inertia. The experimental conditions are then specified, which determine the boundary conditions to be imposed. An impedance head is fixed at the mid-length of the sample giving access to the injected force (white noise type) and velocity at the same point (Fig. 2 (a)). In this configuration, there is a fixation in the middle of the bar length ($L_z/2$) (ensured by gluing a pastille). The observed modal behavior will therefore be equivalent to that of 2 free/semi-rigid bars of length $L_z/2$ (Fig. 2 (b)). The boundary conditions lead to an equation of the form

$$\tan\gamma_n \tanh\gamma_n = 0 \;\; \text{where} \;\; \gamma_n = \beta\frac{L}{2} \quad (5)$$

which is solved graphically. The access to the natural frequencies f_n gives the Young's modulus according to z [11], [12]:

$$E = \frac{3\pi^2}{\gamma_n^4}\frac{\rho L^4}{h^2} f_n^2 \quad (6)$$

where ρ is density, h is thickness, L is length, f is resonant frequency, γ_n depends on boundary conditions. Compared to static tests, this technique has the advantage of being non-destructive. On the other hand, only the Young's modulus in the longitudinal direction can be determined.

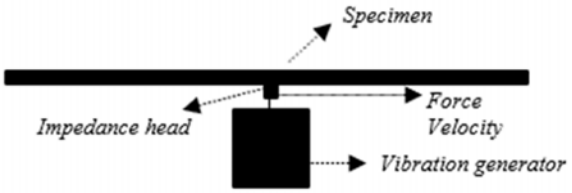

Fig. 2 (a) The experimental IEV set-up [11]

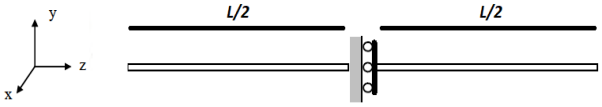

Fig. 3 (b) Boundary conditions

D. Ultrasonic Pulse Velocity (UPV) Testing

Since the beginning of the 19th century, research on wave propagation in elastic solid materials was carried out. UPV tests use elastic (or acoustic) waves as mechanical vibrations which propagate in solids, liquids, and gases. The technique of ultrasound is based on mechanical waves propagating with frequencies above the human hearing range (20 kHz usually) [10]. In addition, at atomic level, there are many different models of vibratory motion, however, in solids there are two modes of bulk wave propagation.

- *Longitudinal waves:* Waves in which particles move in the direction of wave propagation. These are the most rapidly propagating waveforms and are also known as Compression waves or P waves, which are the most relevant to the ultrasound testing of this research.
- *Shear waves:* Also known as transverse waves, where the

direction of vibration is perpendicular to the direction of wave propagation.

The equation of motion can be divided into the following two wave equations (7) and (8) which relate the propagation velocity of a longitudinal wave (V_l) and a shear wave (V_s) to the material density ρ and the two constants used in Hooke's law the Young's modulus E and the Poisson ratio ν (assumed to be equal to 0.25 for both bricks) [10].

$$E = \rho \times V_l^2 \times \frac{(1+\nu)(1-2\nu)}{(1-\nu)} \quad (7)$$

$$G = \rho \times V_s^2 \quad (8)$$

III. Results and Discussion

A. Flexural Tests

Determination of the tensile strength of brittle materials is carried out by means of a 3-points flexural test. The specimens are extracted in three directions, in different parts of the brick A and B. Five specimens are tested for each direction, with dimensions 300 x 20 x 8 for the X, Z and 200 x 20 x 6 for the Y direction (Fig. 3).

The load is applied in the thickness direction. The tests show linear stress-strain relationships and a brittle behavior, represented by a brutal rupture (Fig. 4 (a)). Figs. 5 (a) and (b) show the variation in Young's modulus in the X, Y and Z directions obtained from the flexural and compression tests of bricks A and B: It can be seen that there is a difference between the results in the three directions. Samples extracted in the Z direction (extrusion direction) have the highest values (14.5 GPa for brick A and 10.4 GPa for brick B), which are 50% higher than samples extracted in the X and Y directions for brick A as well as 20% higher than samples extracted in the X and Y directions for brick B. It seems that the reason for the observed anisotropy can be related to the manufacturing process. However, the small difference between the Young's modulus values in the X and Y directions as well as, to simplify numerical modelling later on, the transverse isotropic behavior can be considered [3], [4], [6], [11]. In other words, the elastic properties are approximately the same in the XY plane and are different in the direction perpendicular to this plane.

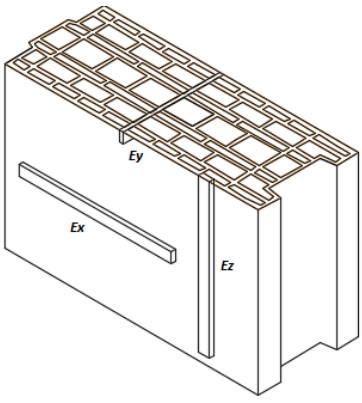

Fig. 3 (a) Extraction directions for test specimens of brick A

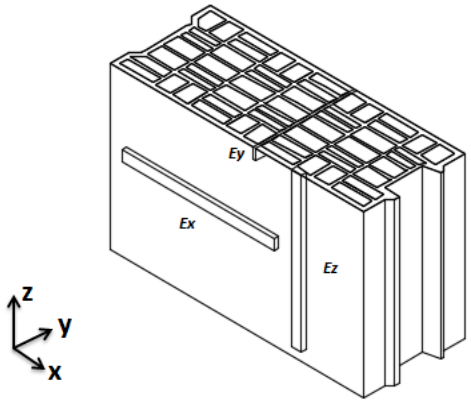

Fig. 3 (b) Extraction directions for test specimens of brick B

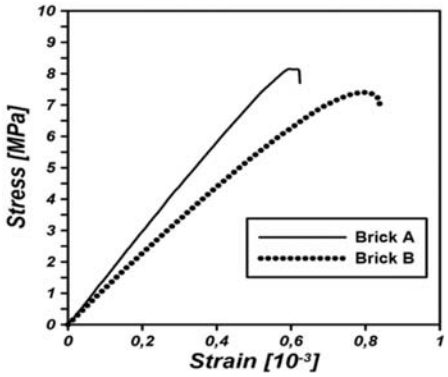

Fig. 4 (a) Stress-Strain curve of the flexural test for the two bricks

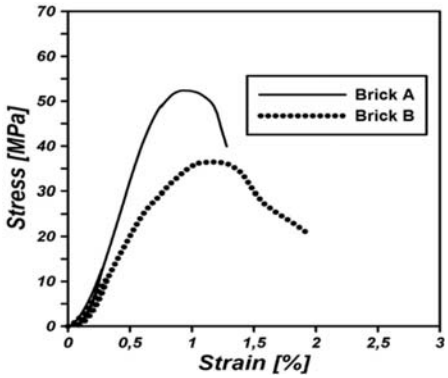

Fig. 4 (b) Stress-Strain curve of the compression test for the two bricks

B. Compression Tests

For the compression tests, the height of the samples should not exceed 6 times their length or width to avoid buckling during the test [8]. Five samples are taken from the internal and external faces of the brick blocks in the three directions, with dimensions of 10 x 10 x 5 mm^3 and 10 x 10 x 8 mm^3 for the X, Z directions for brick A and B as well as 10 x 10 x 3 mm^3 and 10 x 10 x 4 mm^3 for the Y direction for bricks A and B respectively. The loading speed must be low to remain quasi-static and for the test duration to be between 30s-90s [13]. The speed used during those tests is 30 N/s for X, Z directions and 20 N/s for the Y direction in the loading and unloading compression test for brick A and B.

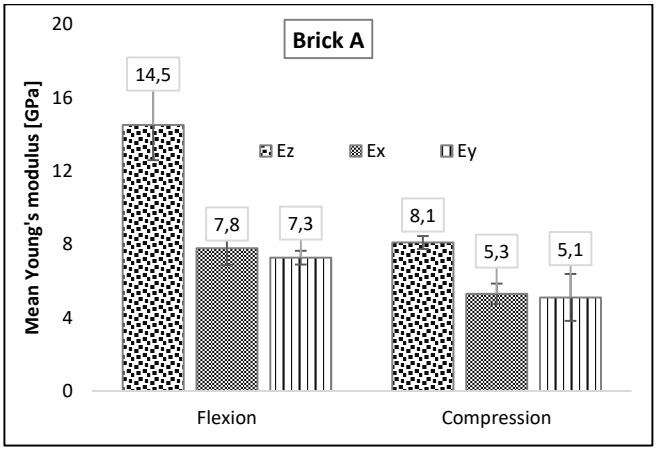

(a)

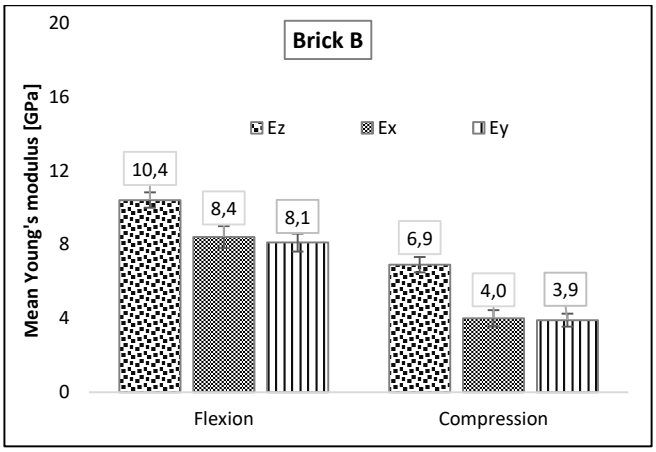

(b)

Fig. 4 (a), (b) Comparison of the mean Young's modulus values in the different directions obtained from the flexural and compression tests of bricks A and B, respectively

The load-unload cycle is performed at stress level of 1/4 of the failure load. These tests allow the acquisition of the stress-strain curves as shown in Fig. 4 (b). This curve initially can be a straight line which shows the elastic behavior then the terracotta begins to show plastic behavior. Abrupt failure is an indication of the brittleness of the material. This behavior is widely used in literature for such material [7], [8]. It is noted that the average compressive strength in the extrusion direction "Z" is 48.6 MPa and 38.8 MPa for bricks A and B, with standard deviations of 2.4 MPa (5%) and 2.7 MPa (7%) respectively. The average compressive strengths in the Z-direction and in the X- and Y-directions differ by 25% and 37% respectively for brick A. Similarly, 9% and 27% differences between the average compressive strengths in the Z-direction and in the X and Y-directions for brick B are indicated. Furthermore, the cyclic loading shows that at the beginning of the unloading, the terracotta is stiffer than in the initial state, i.e., the slope of the unloading curve is greater than the one at the beginning of the curve. This phenomenon can be explained by the fact that the samples contain micro-defects that are forced closed by the mechanical load to make the material more rigid. Thus, Table I presents a summary of the data obtained from the flexural and compression tests for bricks A and B. Note that the mean Young's modulus value is obtained from the loading curves. It indicates that the mean Young's modulus values in the Z direction have the highest values (8.1 GPa for brick A and 6.9 GPa for brick B), which are 35-40% higher than the samples extracted in the X and Y directions for bricks A and B. Furthermore, it is well shown that the mean Young's modulus values in the X and Y directions are the same, which is consistent with the results of the flexural test and may confirm the hypothesis of considering the brick as a transversely isotropic material. Moreover, it is noted that the Young's modulus values obtained in the compression test differ from those of the flexural test in the two bricks. This can be explained by the fact that the elastic deformation of brittle materials such as terracotta may depend on the orientation of the micro-defects which are related to the manufacturing process. As shown in Fig. 6, most of the micro-cracks in the bricks A and B may have the tendency to be in the direction of extrusion. Therefore, in the case of the flexural test, micro-cracks perpendicular to the axis of loading will be forced to be closed, which makes the material more rigid. Otherwise, in the compression test, micro-cracks parallel to the axis of the load will be forced to be opened, leading to a reduction in the stiffness of the material. Therefore, terracotta can be considered as a bimodulus material like some brittle materials used in the literature [14]-[18].

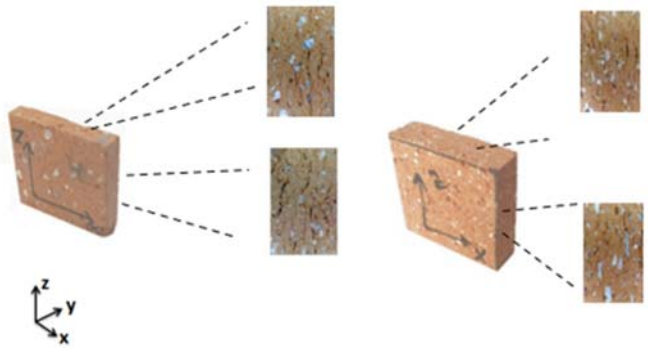

(a) (b)

Fig. 5 Micro-cracks in bricks A and B, respectively, taken by a high-performance camera

TABLE I
SUMMARY OF DATA OBTAINED FROM THE FLEXURAL AND COMPRESSION TESTS FOR BRICK A AND B

Brick	Direction	σ_t (MPa)	σ_c (MPa)	E_t (GPa)	E_c (GPa)
Brick A	X	5.25 - (5%)	36.3 - (16%)	7.8 - (4%)	5.3 - (13%)
	Y	4.3 - (10%)	31.1 - (9%)	7.3 - (8%)	5.2 - (7%)
	Z	8.1 - (5%)	48.6 - (5%)	14.5 - (10%)	8.1 - (10%)
Brick B	X	5.1 - (10%)	35.5 - (3%)	8.4 - (7%)	4.0- (11%)
	Y	4.25 - (8%)	28.5 - (5%)	8.1 - (6%)	3.9 - (9%)
	Z	6.1 - (18%)	38.8 - (7%)	10.4 – (4%)	6.9 – (6%)

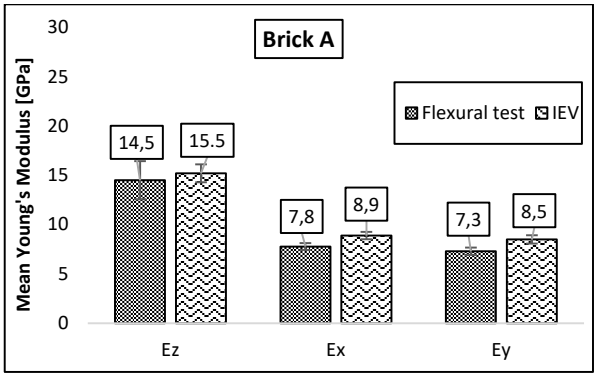

(a)

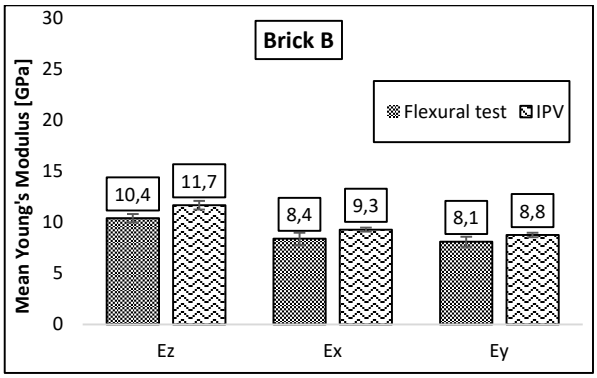

(b)

Fig. 6 Comparison between the mean values of Young's modulus obtained from the flexural and IEV test for bricks A and B, respectively

C. Impulse Excitation of Vibration (IEV) Testing

Using the impulse excitation method, the dynamic Young's modulus is computed based on the measured resonance frequencies of the flexural vibration of the brick samples. The non-destructive character is one of the main advantages of this method. It is therefore used prior to the flexural test. The same specimens mentioned in Section III *A* are used (Fig. 3). A difference of approximately 10% between the mean values of Young's modulus obtained from the static and dynamic test for all directions is shown in Fig. 7 for the two bricks. The difference is mainly explained by the fact that the strain values in static tests are higher than in dynamic tests. Besides, in static tests, samples of the brick containing micro-cracks react to changes in stress by opening or closing, which affects Young's modulus as mentioned above [19]. On the contrary, the propagation of an elastic wave of sufficiently high frequency is not impacted by cracks [20]-[22]. In addition, according to the literature on materials similar to brick, the degree of compaction of the material during the manufacturing process influences the results. Thusly, the more compact the material, the better the match between the static and dynamic moduli [19]. If the material is slightly damaged, matching may still happen, but only for the low-stress parts of the static tests, since crack closure does not yet have a clear effect on the stress-strain curve [19]. This can be confirmed by analogy with engineering practice, according to which very compact materials are thoroughly examined using a static and dynamic approach and the results are identical [23]. Furthermore, the difference between the static and dynamic moduli increases with increasing damages to the brittle material in the case of less compact materials with a non-linear stress-strain relationship [24].

D. UPV Testing

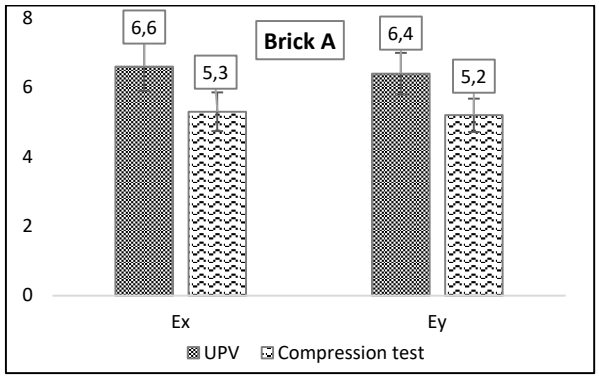

(a)

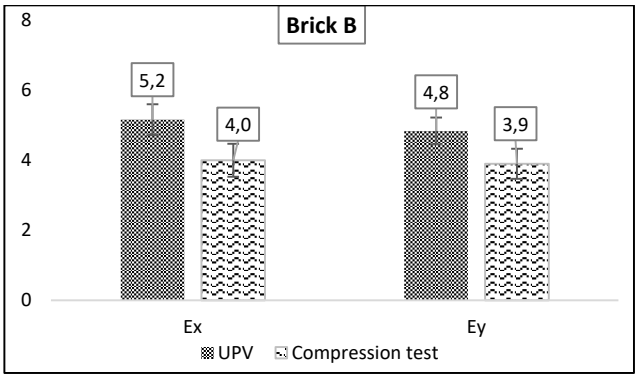

(b)

Fig. 7 Comparison between the mean values of Young's modulus obtained from the UPV and compression tests for brick A and B, respectively

The travel times of the ultrasonic pulses were measured using a commercial ultrasonic tester PROCEQ Pundit. It integrates a receiver amplifier, a pulse generator, and a time measurement circuit. The same specimens used in IEV test for the two bricks are used. In addition, a coupling gel was added between the transducers and the material during the tests, as well as the surfaces of the specimens were initially rectified to assure a smooth surface to avoid the loss of excessive signal caused by inadequate acoustic coupling. As with the IEV tests, the humidity level of the specimens is a factor that can affect the results of the UPV. Therefore, measurements were performed on samples stored at room temperature for 48 hours to control this parameter. The mass and dimensions measured for the IEV tests were used, prior to the UPV test, in order to calculate the sample density necessary to determine the dynamic Young's modulus using (7). As bricks are known to exhibit a significant level of anisotropy so a determination of the impulse velocity at several locations and even in different

directions is important. On the other hand, due to the small thickness of the internal and external partitions of the brick (3-9 mm), which does not correspond to the transducer size, only the dynamic Young's modulus in the X and Y directions are measured. Fig. 8 presents a good agreement between the static Young's modulus obtained from the compression test and the dynamic Young's modulus obtained from UPV for brick A and B.

IV. Conclusion

The simple compression and flexural tests carried out at room temperature allow a better understanding of the mechanical behavior of the considered material. The comparison between the non-destructive and destructive tests also gives interesting conclusions.

- The Young's modulus values obtained in the compression test are lower than those obtained in the flexural test. This was explained by the fact that the elastic deformation of brittle materials such as terracotta depends on the orientation of micro-defects related to the manufacturing process. It is necessary to take this difference into account in numerical modelling by considering terracotta as a bimodulus material.
- In the flexural test, The Young's modulus values vary depending on the direction considered. Samples extracted in the Z direction (extrusion direction) have the highest values compared to the X and Y directions. This is due to the anisotropy of the material inherited from the extrusion process. Also, due to the small difference between the Young's modulus values in the X and Y directions, the transverse isotropic behavior can be considered later on for terracotta, which simplifies the numerical modelling, compared to the anisotropic one.
- There was a difference of approximately 10% between the mean Young's modulus values obtained from the flexural and IEV tests for all directions. This difference is mainly due to the fact that in the static tests, the samples containing micro-defects react to changes in stress by opening or closing, which affects Young's modulus. In contrast, the propagation of an elastic wave of sufficiently high frequency is not affected by micro-defects randomly distributed.
- A good agreement between the values of the Young's modulus is obtained from the compression and UPV tests.

Moreover, since this paper deals with one of the elementary components of masonry walls, it is necessary to continue to study the mechanical characterization of other masonry wall components such as thin joints and coatings at both room and high temperatures to fully understand the fire behavior of masonry walls. In addition, this paper can also be extended to develop a damage model for brick that takes into account the bimodulus transversely isotropic behavior.

Acknowledgment

The project received financial and material support from CTMNC – Technical Center of Natural Building Material, France.

References

[1] S. Ahmed, and B.D. Hachmi "A Multi-Physics and Multi-Scale Approach for Hollow Clay-Brick Masonry." 2015.
[2] N. Thê-Duong, and M. Fekri. "Behavior of hollow clay brick masonry walls during fire. Part 2: 3D finite element modeling and spalling assessment." Fire Safety Journal 66 (2014): 35-45.
[3] P. B., Lourenço, G. Vasconcelos, P. Medeiros, and J. Gouveia. "Vertically perforated clay brick masonry for loadbearing and non-loadbearing masonry walls." Construction and Building Materials 24, no. 11 (2010): 2317-2330.
[4] G. Jacqus, S. Berger, G. Vincent, J. Philippe, V. Michel, and C. Sébastien. "A homogenised vibratory model for predicting the acoustic properties of hollow brick walls." Journal of Sound and Vibration 330, no. 14 (2011): 3400-3409.
[5] Z. Svoboda, and K. Marek. "Numerical simulation of heat transfer through hollow bricks in the vertical direction." Journal of Building Physics 34, no. 4 (2011): 325-350.
[6] K. Michel. Clay bricks and rooftiles, manufacturing and properties. lasim, 2007.
[7] N. The-Duong. Etude du comportement au feu des maçonneries de briques en terre cuite : Approche expérimentale et modélisation du risque d'écaillage. PhD thesis, Université Paris-Est, 2009.
[8] S. Ahmed. "Modélisations thermomécanique et numérique du comportement de maçonneries en briques alvéolées en terre cuite sous chargements mécanique et thermique sévères." PhD diss., 2018.M. Young, *The Techincal Writers Handbook.* Mill Valley, CA: University Science, 1989.
[9] D.B., Emmanuel, E. Blond, M. Christine, C. Thierry, N. Schmitt, and J. Poirier. "Identification du module d'Young de matériaux réfractaires à base SiC." In Matériaux 2010, p. CD. 2010.
[10] N. Makoond, P. Luca and M. Climent. "Dynamic elastic properties of brick masonry constituents." Construction and Building Materials 199 (2019): 756-770.
[11] G. Jacqus,. "Etude des caractéristiques acoustiques des matériaux alvéolaires utilisés pour la construction de parois dans le bâtiment." PhD diss., Université de Toulouse, Université Toulouse III-Paul Sabatier, 2011.
[12] D. Abdelhakim, and Z. Abdellatif. "Identification of elasticity modulus by vibratory analysis (Application to a natural composite: Aleppo pine wood)." In MATEC Web of Conferences, vol. 149, p. 01045. EDP Sciences, 2018.
[13] NF EN 1015-11. Méthodes d'essai des mortiers pour maçonnerie - Partie 11 : détermination de la résistance en flexion et en compression du mortier durci, Septembre 2000
[14] D. Zongliang, Z. Yupeng, Z. Weisheng, and G. Xu. "A new computational framework for materials with different mechanical responses in tension and compression and its applications." International Journal of Solids and Structures 100 (2016): 54-73.
[15] A. Zolochevsky, E. Yeseleva, and W. Ehlers. "An anisotropic model of damage for brittle materials with different behavior in tension and compression." Forschung im Ingenieurwesen 69, no. 3 (2005): 170-180.
[16] T. You, Z. Qi-Zhi, L. Peng-Fei, and S. Jian-Fu. "Incorporation of tension-compression asymmetry into plastic damage phase-field modeling of quasi brittle geomaterials." International Journal of Plasticity 124 (2020): 71-95.
[17] H. Eli S., A.C. José A., L. Alexis, and J.M. John. "Modeling of Bimodulus Materials with Applications to the Analysis of the Brazilian Disk Test." 2019
[18] D. Zongliang, Z. Weisheng , Z. Yupeng, X. Riye , and G. Xu. "Structural topology optimization involving bi-modulus materials with asymmetric properties in tension and compression." Computational Mechanics 63, no. 2 (2019): 335-363.
[19] C. František, V. Jan, P. Matìj and B. Zita. "Determination of static moduli in fractured rocks by T-matrix model." Acta Montanistica Slovaca 22, no. 1 (2017).
[20] P.N., Laura J., and N. David D. "Frequency dependence of fracture stiffness." Geophysical Research Letters 19, no. 3 (1992): 325-328.
[21] M.H. Worthington. "Interpreting seismic anisotropy in fractured reservoirs." First Break 26, no. 7 (2008): 57-63.
[22] V. Jan, R. Vladimír, L. Tomáš, and Z. Roman. "Velocity dispersion in fractured rocks in a wide frequency range." Journal of Applied

Geophysics 90 (2013): 138-146.
[23] L. Hassel. "Dynamic vs. static Young's moduli: a case study." Materials Science and Engineering: A 165, no. 1 (1993): L9-L10.
[24] P. Antonio, C. Giovanni B., F. Nicoletta, and C. Riccardo. "General characterization of the mechanical behaviour of different volcanic rocks with respect to alteration." Engineering geology 169 (2014): 1-13.